Deformation Behavior of Sphere-Forming Trifunctional Multigraft Copolymer

Yongxin Duan,[†,§] Erik Rettler,[‡] Konrad Schneider,[§] Ralf Schlegel,[†] Mahendra Thunga,[†,§] Roland Weidisch,*[,†,§] Heinz W. Siesler,[‡] Manfred Stamm,[§] Jimmy W. Mays,[||] and N. Hadjichristidis[⊥]

Institute of Materials Science and Technology (IMT), Friedrich-Schiller-University Jena, Löbdergraben 32, D-07743 Jena, Germany; Department of Physical Chemistry, University of Duisburg-Essen, Schützenbahn 70, D 45117 Essen, Germany; Leibniz-Institute of Polymer Research Dresden, Hohe Strasse 6, D-01069 Dresden, Germany; Department of Chemistry, University of Tennessee, Knoxville, Tennessee 37996; and Department of Chemistry, University of Athens, Athens, Greece

Received May 7, 2008
Revised Manuscript Received June 5, 2008

Introduction. Recently, a series of multigraft (MG) polystyrene-*g*-polyisoprene (PS-*g*-PI) copolymers, with controlled molecular weight of the backbone and the graft arm, the arm polydispersity, number of branch points, and the number of arms grafted to each branch point, were synthesized successfully by Mays et al.[5–8] Preliminary studies have shown that multigraft PS-*g*-PI copolymers with ca. 20 wt % PS, and regular spaced junction points, without respect to different functionality (tri-, tetra-, and hexafunctionality) and microphase morphology (PS spheres, cylinders, and lamella) have exceptional elasticity compared to commercial thermoplastic elastomers (TPE).[1–3] Multigraft copolymers stretched up to about 1400% show a residual strain of 40% only, not yet reached by any TPE. For understanding the origin or mechanism of such exceptional elasticity, named as superelasticity, more detailed studies are required. In this paper we studied the deformation behavior of sphere-forming trifunctional MG copolymer by synchrotron SAXS and rheo-optical FT-IR on nanometer size scales and molecular level, respectively.

Previous deformation studies on sphere-forming copolymers are mostly performed on linear block copolymers.[9–13] Beecher et al. studied the deformation process of SBS triblock copolymers by TEM.[9] The basic morphological unit is PS sphere of 120 Å diameter dispersed in a matrix of PB. They found that, upon stretching, the PS particles become ellipsoidal, eventually highly elongated, approaching the length of the fully extended PS segment. And further elongation leads to cohesive failure of the PS particles. They attributed this ductility to the greater degree of freedom of PS segments in the vicinity of the interface. But they did not pay attention to another important component: PB phase. The second study on the deformation mechanism of sphere-forming block copolymer was performed by Hashimoto et al.[10] by combining light scattering, SAXS, and TEM. Contrary to the previous study, they found that the spherical domains of the styrene component are hardly deformed. The SAXS data indicate that the change in interdomain spacing becomes nonaffine at strains above 10%. Changes in light scattering patterns are attributed to the appearance of density fluctuations at lower strains and void formation at higher strains. TEM micrographs of the stretched specimens also show regions of low concentration of spherical domains. Of particular interest, Séguéla et al. studied the deformation behavior of a polybutadiene-hydrogenated SBS and found that the deformation of this material is highly affine until the upper draw ratio of 2.3.[11] Accordingly, this sphere-forming block copolymer was considered as model system for applying a general relation proposed for testing the affinity of grain deformation in mesomorphic block copolymers. Recently, Takahashi et al. studied the elongational behavior of sphere-forming SIS triblock copolymers by SAXS and FT-IR.[4] The lattice deformation examined by SAXS for $\lambda < 3$ can be well expressed by affine deformation, and FTIR examination showed that PI segments have obvious orientation along the stretching direction, while the deformation of PS is negligibly small compared to that of elastic PI chains.

Obviously, there is no commonly accepted concept about the deformation mechanism of sphere-forming block copolymers. The controversy focuses on two points: the deformation is affine or nonaffine, and PS microdomains are deformable or not. In this communication, sphere-forming trifunctional MG sample is submitted to uniaxial tensile deformation experiment, and the evolution of the microdomain structure is examined by SAXS measurement, while deformation at the local molecular segmental level is investigated by the simultaneous in situ microscopic infrared dichroism measurement during stretching. We hope this research can shed more light on the above-mentioned topic.

Experimental Part. The sample used in this investigation is a trifunctional MG copolymer based on PI backbone and PS branches with average 2.6 branch points spaced regularly along the backbone (Figure 1). The PS content is 19 wt %. The weight-average molecular weight of the whole molecule and PS arm is 391 and 31.6 kg/mol, respectively. The synthesis of trifunctional MG copolymers was described by Iatrou et al.[7,8]

The preparation of samples for SAXS and FITR characterization was described in our previous publications.[1–3] The thickness of the sample is maintained at 30−40 μm for FT-IR studies whereas it is 200 μm for SAXS investigations.

Synchrotron SAXS measurement at room temperature was performed at the Deutsches Elektronen-Synchrotron (DESY) in Hamburg. The wavelength and sample−detector distances were 0.138 nm and 7880 mm, respectively. A homemade stretching device[14,15] was used to measure SAXS at constant strain, which was determined from in situ recorded images of the sample during deformation by a digital camera. The design of the stretching machine allows the sample to be uniaxially stretched by equal amounts from the center of the sample. Only the central part of the sample was irradiated by the X-ray beam.

Figure 1. Illustration of MG copolymer based on PI backbone and PS branches with regularly spaced trifunctional junction points.

* Corresponding author: E-mail: roland.weidisch@uni-jena.de, Fax +49-3641-947702.
[†] Friedrich-Schiller-University Jena.
[‡] University of Duisburg-Essen.
[§] Leibniz-Institute of Polymer Research Dresden.
[||] University of Tennessee.
[⊥] University of Athens.

10.1021/ma801036y CCC: $40.75
Published on Web 06/14/2008

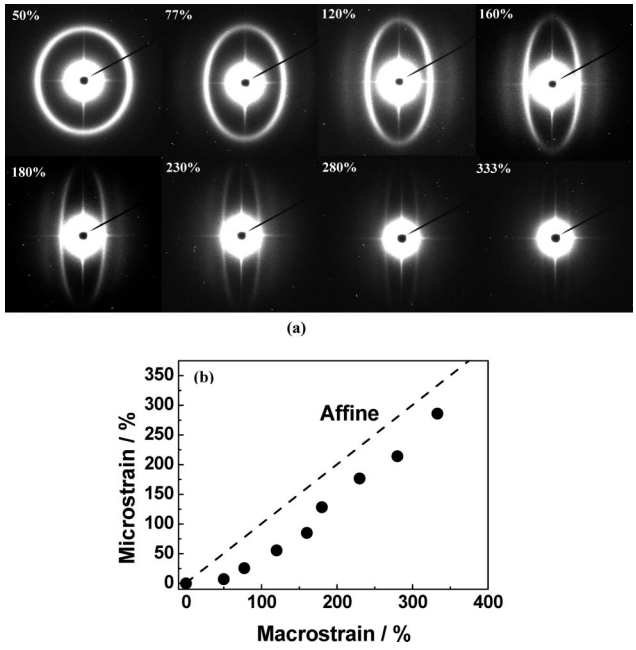

Figure 2. (a) 2-D SAXS patterns at different strains; the stretching direction is horizontal. (b) Microstrain plotted as a function of macrostrain.

The rheo-optical FT-IR measurements were carried out by employing a computer-controlled electromechanical film-stretching device[16] mounted in the sample compartment of a Bruker IFS88FTIR spectrophotometer. The sample films with gauge dimensions of 7×4 mm^2 and a thickness of 30−40 μm were uniaxially stretched at constant strain rate of 3.2 mm/min. Spectra were measured using alternatively parallel and perpendicular polarized IR radiation. A pneumatically rotatable wire-grid polarizer (SPECAC) controlled by the computer adjusted the polarization direction of the incident radiation parallel and perpendicular to the stretching direction by a rapid 90° rotation. The change of the polarization direction is automatically initiated by the last scan of each spectrum. Ten scans per spectrum were accumulated, and the spectral resolution was 4 cm^{-1}. A specially designed software[17] was developed to manage the large number of spectra collected during a rheo-optical experiment.

Results and Discussion. Figure 2a shows the 2-D SAXS patterns at different strains. The presence of single first-order scattering at 0% strain (not shown here) indicates the presence of phase-separated morphology, and this morphology is confirmed to be spherical morphology by TEM investigation in one of our recent publication.[3] Upon stretching, the initial circular scattering pattern becomes elliptical with its major axis perpendicular to the stretching direction (SD). The scattering peak along SD moves toward the origin while that perpendicular to SD moves from the origin with increase of strain. Change of the 2-D SAXS indicates that the average interdomain distance along SD was increasing with a simultaneous decrease of that in the direction perpendicular to SD. The intensity of the scattering in the perpendicular direction is observed to decrease gradually, and the scattering eventually disappears at high deformation. Another obvious change of the 2-D pattern is the appearance of the second scattering from 77% of strain. With increase in the deformation the intensity of this second-order peak is gradually increasing, and its position was coming closer toward smaller scattering angle.

Different explanations are given for the origin of such second-order scattering which appears in the SAXS pattern during deformation process. Hashimoto et al. studied the deformation behavior of sphere-forming SI and SIS[10] and concluded that the second peak was related to the single-domain scattering, and its position is only affected by the radius of PS spheres. In our study the second peak move toward the origin; it seems that the PS spheres are deformed. But from Figure 2a, we can find that the intensity of the second scattering increases upon stretching (from 77% to 160% strain). If this peak is only related to the size of PS spheres, its intensity should be kept unchanged or decrease during deformation due to the decrease of sample thickness. Séguéla and Prud'homme proposed this peak is from lattice reflection.[11] For undeformed material, this peak coincides with minimum of the particle scattering, so it is obscured in the initial SAXS pattern. Therefore, it seems that the change of our SAXS pattern with stretching is similar to Séguéla's study, and the second scattering can be assigned to the lattice reflection. But there is a possibility that this scattering is a combination of lattice reflection and single particle scattering. For clarifying this issue, it is necessary for us to perform TEM study on deformed sample. We will report this elsewhere.

According evolution of the first-order diffraction, the microstrain, also called as Bragg spacing strain, can be calculated with $\varepsilon_{mi} = (d_1 - d_0)/d_1$. In Figure 2b, microstrain is plotted as a function of macrostrain (macroscopically change of the sample length) calculated according to optical pictures captured during measurement. The linear fit of the data gives a slope of 0.86. It is quite close to affine deformation. But all of microstrain values are smaller than that expected from affine deformation. As to our knowledge, this kind of deformation behavior has never been reported. At first we need exclude the possibility of the

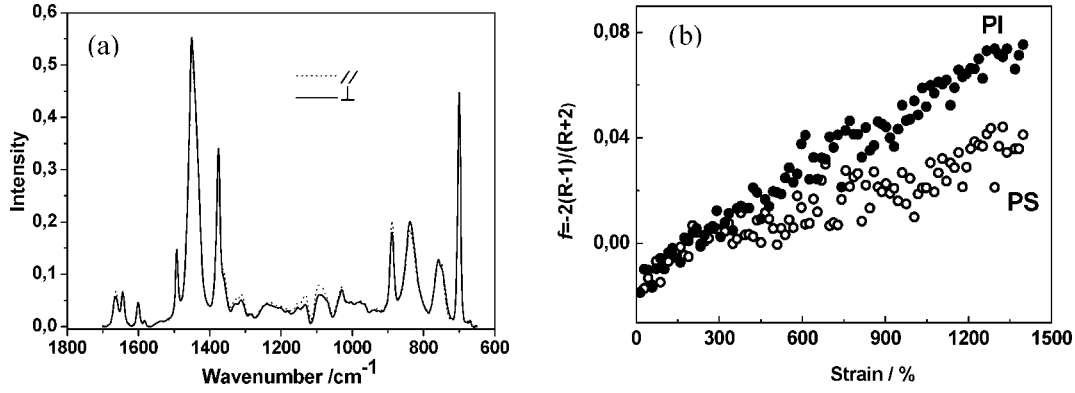

Figure 3. (a) Polarized FTIR spectra of trifunctional MG copolymer stretched to 1500% of strain. (b) Strain dependence of orientation function for PI and PS component.

under-evaluation of the microstrain. We evaluated the deformation process of other tri- and tetrafunctional MG copolymers, which were examined with the same synchrotron SAXS source, drawing machine, experiment conditions, and same evaluation method. For trifunctional MG copolymers, the same result was obtained, but for tetrafunctional MG copolymers, perfect affine deformation was found. So the result is reliable. The difference of deformation behavior betwenn tri- and tetrafunctional MG copolymers should be from the difference of their molecular architecture. In the future work we will give explanation to this unusual deformation behavior.

Figure 3 (a) shows the polarized FTIR spectra of trifunctional MG copolymer stretched to 1500% of strain with the electric vector parallel (∥) and perpendicular (⊥) to SD. It is found that there is small but obvious difference between these two spectra. The bands at 1376, 1493, and 1601 cm^{-1} have lower absorbance at the spectrum with the vector parallel to SD, and the band at 888 cm^{-1} has lower absorbance at the spectrum with the vector perpendicular to SD. In order to study the deformation mechanism of MG copolymers on their molecular level, infrared dichroism analysis is employed.[18] The infrared dichroism allows one to determine orientation function (1). Here, R represents the dichroic ratio which is given by $R = A_{\parallel}/A_{\perp}$ (with $A_{\parallel}$ and $A_{\perp}$ the absorbances of specific absorption bands measured with IR radiation polarized parallel and perpendicular to the SD, respectively); $R_0 = 2\cot^2\psi$, where ψ is the angle between the chain axis and the transition moment of the infrared vibration considered.

$$f = \frac{(R_0 + 2)(R - 1)}{(R_0 - 1)(R + 2)} \tag{1}$$

For the infrared vibration with transition moment parallel to the chain axis, eq 1 can be written as eq 2. When the transition moment of the infrared vibration is perpendicular to the chain axis, eq 3 can be obtained.

$$f = \frac{R - 1}{R + 2} \tag{2}$$

$$f = -2\frac{R - 1}{R + 2} \tag{3}$$

The magnitude of f is directly proportional to the degree of orientation.

As observed from the SAXS and TEM investigations, the investigated MG copolymer has a heterogeneous phase-separated structure with spherical morphology. The collective deformation from the heterogeneous phases is characterized by observing the selective orientation in the individual phases. For quantitative evaluation, the absorption bands at 1376 and 1493 cm^{-1} are selected for PI and PS phases, respectively. The band at 1376 cm^{-1} is assigned to the symmetric vibration of CH_3, while the band at 1493 cm^{-1} can be assigned to a C−H in plane stretching mode. The transition moment of both bands is assumed to be about 90° with respect to the PI and PS chain axis, respectively. So eq 3 is used to calculate orientation function value of the bands at 1376 and 1493 cm^{-1}. This means an increase of f value corresponds to an increase in orientation and vice versa.

Figure 3b shows the orientation function value from selective bands vs strain. At smaller strains, i.e. below 300% of strain, the f value of 1376 (f_{PI}) and 1493 cm^{-1} (f_{PS}) shows a similar trend in their strain dependence and increase with the increase of strain. From 400% strain, f_{PS} has a mild increase while f_{PI} keeps the same slope as that at low strain, but the value of f_{PS} is comparable with that of f_{PI}. And obviously it can be observed that even at larger strains, i.e., above 1200%, the values of both

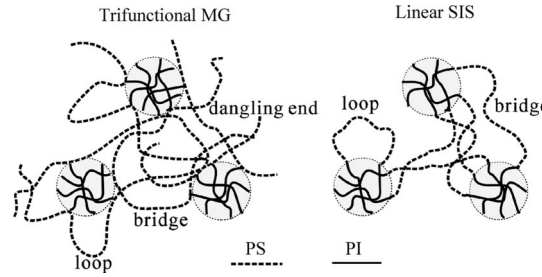

Figure 4. Difference in molecular architecture and conformation between trifuctional MG and linear SIS.

f_{PI} (0.07) and f_{PS} (0.04) are comparable and quite small when compared to the value for the perfect orientation ($f = 1$), which reveals that, upon stretching, both PS and PI segments aligned slightly along SD.

The evolution of f_{PS} and f_{PI} in trifunctional MG copolymer is quite abnormal when compared to linear triblock copolymers (SIS) because, in general, the modulus of PI phase is much smaller than that of PS phase and the f_{PI} value is much bigger than the f_{PS} value. For example, in linear triblock copolymers, f_{PI} is about 0.2 at 500% strain and f_{PS} value is negligibly small compared to that of elastic PI chains.[4] In order to explain the lower orientation of the PI phase in MG copolymer than that in SIS, it is necessary to pay attention to the difference in molecular architecture and conformation between them. As shown in Figure 4, for a linear triblock copolymer, both ends of the central PI segment are connected to PS segments, whereas for the MG copolymer, there are two kinds of PI segments: one kind of PI segment has two ends connected with other PI segments and PS branches; another kind of PI segment with one end is connected with other segments and another end is free. In the bulk state, PI segments of SIS can form either bridges or loops, and that of MG copolymer can form bridges, loops, and dangling ends. In general, during the deformation process the PI segments with bridge conformation can be easily stretched when compared to dangling ends. Even in some cases the dangling PI segments are stretched, they can relax quite fast due to one free end. Daoulas et al.[19] have calculated the relaxation time of PI dangling ends of SI diblock copolymer and found that it is of the order of 150 s at room temperature. This time scale is much shorter compared to the whole stretching process of the FT-IR measurement (ca. 15 min). As shown in Figure 4 in trifunctional MG with ∼3 branch points (2.6 number of branch points in the present MG copolymer samples), about half of the PI segments can form either bridge or loop conformation similar to SIS triblock copolymers and can be stretched effectively during the deformation process, whereas the other half of PI segments which have one dangling end cannot be stretched effectively or oriented along SD. As stated by Kennedy, the dangling-end segments do not contribute to the load-bearing capability of the TPE but act as useless diluents.[20] It was also reported earlier that for sphere-forming SIS triblock copolymers due to the coexistence of loops along with the bridge type conformation, the bridging fraction is observed to be 75%−80%,[21] which means that around 75%−80% of PI segments can be stretched effectively and oriented along the SD. In the present scenario, one can observe that only 50% of the PI segments are contributing for formation of both bridge and loop type conformation; then less than 50% of the PI segments form bridge type conformation and can be stretched during stretching process which is due to the coexistence of loop type conformation within this 50% of PI segments.

As the observed f_{PI} value from the rheo-optical FT-IR studies is the average value of all kinds of PI segment in the bulk sample, it is quite obvious to expect a smaller value of f_{PI} for MG copolymer when compared to SIS triblock copolymers.

Similar evolution of f_{PS} and f_{PI} with increase of strain and comparable value means that PS and PI phases deform in similar manner and stress is effectively transformed between two phases. In trifunctional MG copolymer one PS segment is connected with two PI segments while in SIS one PS segment is connected with only one PI segment. If trifunctional MG copolymer and SIS with same length of PS segments form PS domains with same number of PS chains, the number of PI chains connected to one PS domain (we defined it as functionality of PS domain) in trifunctional MG copolymer will be double to that in SIS (Figure 4). Such doubled functionality of PS domains caused by the special molecular architecture of trifunctional MG copolymer may improve dramatically the effectiveness of the stress transformation between two phases. And the deformability of PS domains is highly related to the morphology of the trifunctional MG copolymer. The morphology in the studied copolymer is PS spheres dispersed in the PI matrix. Styrene segments in the vicinity of the interface will have a greater degree of freedom than those in the interior. Greater mobility and lower transition temperature for these styrene units in the vicinity of the interface can be expected. A consequence of this mobility is the ductility of the PS phase; on stretching (even at temperature far below the T_g of PS), the PS particles are deformed and PS chains become oriented along the stretching direction.

Conclusion. We examined the elongation behavior of sphere-forming trifunctional MG copolymer. The average interdomain distance along SD increases while that perpendicular to SD decreases. The second scattering appears during deformation, and its origin can be attributed to either the lattice reflection or combination of lattice reflection and single particle scattering. All of microstrain values evaluated form SAXS pattern are smaller than that expected from affine deformation. From rheo-optical FT−IR studies it was found that both PS and PI phases were stretched in a similar manner, and stress can be transformed effectively between the two phases, which is explained by the doubled functionality of PS domains and coexistence of bridge, loop, and dangling PI chains due to the special molecular architecture of MG. This verified the speculation on the origin of superelasticity in our former study.

Acknowledgment. Y. X. Duan is grateful to the Alexander von Humboldt foundation for kindly providing the fellowship in Germany which made it possible for her to perform this study. The authors thank Mr. Torsten Hofmann for his kind help for SAXS measurements.

References and Notes

(1) Weidisch, R.; Gido, S. P.; Uhrig, D.; Iatrou, H.; Mays, J.; Hadjichristidis, N. *Macromolecules* **2001**, *34*, 6333–6337.
(2) Staudinger, U.; Weidisch, R.; Zhu, Y.; Gido, S. P.; Uhrig, D.; Mays, J.; Iatrou, H.; Hadjichristidis, N. *Macromol. Symp.* **2006**, *233*, 42–50.
(3) Zhu, Y. Q.; Burgaz, E.; Gido, G. P.; Staudinger, U.; Weidisch, R.; Uhrig, D.; Mays, J. *Macromolecules* **2006**, *39*, 4428–4436.
(4) Takahashi, Y.; Song, Y.; Nemoto, N.; Takano, A.; Akazawa, Y.; Matsushita, Y. *Macromolecules* **2005**, *38*, 9724–9729.
(5) Gido, S. P.; Lee, C.; Pochan, D.; Pispas, S.; Mays, J. W.; Hadjichristidis, N. *Macromolecules* **1996**, *29*, 7022–7028.
(6) Xenidou, M.; Beyer, F.; Hadjichristidis, N.; Gido, S. P.; Beck Tan, N. *Macromolecules* **1998**, *31*, 7659–7667.
(7) Xenidou, M.; Hadjichristidis, N. *Macromolecules* **1998**, *31*, 5690–5694.
(8) Iatrou, H.; Mays, I. W.; Hadjichristidis, N. *Macromolecules* **1998**, *31*, 6697–6701.
(9) Beecher, J. F.; Marker, L.; Bradford, R. D.; Aggarwal, S. L. *J. Polym. Sci., Part C* **1969**, *26*, 117–134.
(10) Inoue, T.; Moritani, M.; Hashimoto, T.; Kawai, H. *Macromolecules* **1971**, *4*, 500–507.
(11) Séguéla, R.; Pru'homme, J. *Macromolecules* **1988**, *21*, 635–643.
(12) Prasman, E.; Thomas, E. L. *J. Polym. Sci., Part B: Polym. Phys.* **1998**, *36*, 1625–1636.
(13) Richards, R. W.; Welsh, G. *Eur. Polym. J.* **1995**, *31*, 1197–1206.
(14) Schneider, K.; Trabelsi, S.; Zafeiropoulos, N. E.; Davies, R.; Riekel, C.; Stamm, M. *Macromol. Symp.* **2006**, *236*, 241–248.
(15) Davies, R. J.; Zafeiropoulos, N. E.; Schneider, K.; Roth, S. V.; Burghammer, M.; Riekel, C.; Kotek, J. C.; Stamm, M. *Colloid Polym. Sci.* **2004**, *282*, 854–866.
(16) Siesler, H. W. *Makromol. Chem., Macromol. Symp.* **1992**, *53*, 89–95.
(17) Kalkar, A. K.; Siesler, H. W.; Pfeifer, F.; Wadekar, S. A. *Polymer* **2003**, *44*, 7251–7264.
(18) Zhao, Y. *Macromolecules* **1992**, *25*, 4705–4711.
(19) Daoulas, K.; Theodorou, D. N.; Roos, A.; Creton, C. *Macromolecules* **2004**, *37*, 5093–5109.
(20) Kennedy, J. P. Thermoplastic Elastomers By Carbocationic Polymerization. In *Thermoplastic Elastomers*, 2nd ed.; Holden, G., Legge, N. R., Quirk, R., Schroeder, H. E., Eds.; Hanser: Muinch, 1996; p 369.
(21) Matsen, M. W.; Thompson, R. B. *J. Chem. Phys.* **1999**, *111*, 7139–7146.

MA801036Y